JOURNAL OF MATERIALS SCIENCE 31 (1996) 795–805

Spinel growth in the interface of δ-Al_2O_3 fibre reinforced aluminium piston alloys

H. J. DUDEK, R. BORATH
DLR, Institute for Materials Research, 51 140 Köln, Germany
A. KLEINE
BAFA Federal Export Office, 65 726 Eschborn, Germany

Spinel growth is studied by analytical electron microscopy in the fibre–matrix interface of as-processed and in thermal treated δ-Al_2O_3 fibre reinforced AlSi12CuMgNi alloys. In the as-processed composites a few nanometer large spinel crystals are observed in the fibre–matrix interface. They are interpreted as the reaction product of remnants of the SiO_2 binder, with magnesium segregating in the interface. In the thermally treated material, large spinel crystals of a few tenths of a micrometer grow on the fibre, preferentially at positions where α-Al_2O_3 crystals reach the δ fibre surface. The spinel grows into the aluminium grain of the matrix, as well as into α-Al_2O_3 of the fibre. The orientational relationship of the spinel and the alumina is studied and the results are discussed in relation to the fibre wetting, adhesion and fibre–matrix reaction.

1. Introduction

Wetting and adhesion in Al_2O_3 fibre reinforced aluminium alloys was considered to be connected with the development of a "mono-atomic" layer of an $MgAl_2O_4$ spinel in the fibre–matrix interface [1, 2]. Some experimental results prove this assumption. A monolayer of magnesium was found in the fibre–matrix interface [3, 4] and electron diffraction experiments show spinel structures [2] in as-processed composites. In thermally treated composites large spinels are growing, preferentially on the α-Al_2O_3 crystals of the δ fibre [5]. Wetting and adhesion is, however, also observed in composites without magnesium additives, and in wetting experiments of pure aluminium on alumina wetting angles of 80° (at temperatures above 1000 °C) [6, 7] with adhesion energies typical of chemical bonding are observed [8]. Wetting of aluminium alloys to alumina, on the other hand, is promoted by the addition of magnesium to the alloy, as shown by wetting experiments [9] and as found in processing composites by squeeze casting [5].

The reaction of an aluminium–magnesium alloy melt with alumina fibres resulting in the formation of small spinel crystals at the fibre–matrix interface as a reaction product was studied by several authors. A short review is given in [10]. In principle, spinel as well as magnesia can be formed in such systems. The formation of magnesia or spinel are competitive processes with the preferential formation of spinel at low magnesium concentrations [10] and low oxygen partial pressures in the alloy [11].

The δ-Al_2O_3 fibre (Saffil^R, ICI) consists of approximately 3 wt % SiO_2 for the stabilization of δ-Al_2O_3. The δ- and γ-Al_2O_3 of the δ fibre has a grain size of a few tens of nanometers. The fibre preform is usually bonded using an SiO_2 binder. The thermodynamical stability of SiO_2 is much lower than that of Al_2O_3 [12, 13] and the interaction speed of magnesium with SiO_2 is much higher than with the Al_2O_3. Composites processed with fibres having a high SiO_2 content, e.g. aluminosilicate fibres, are therefore less stable than those with the δ-Al_2O_3 fibre [5]. SiO_2 of these fibres is reduced by molten aluminium at infiltration temperatures [14] (a similar reaction as in the Al–SiO_2 system, is observed also in Al–Al_2O_3 system for temperatures above 1000 °C [7, 15]). Reaction of SiO_2 with the melt is considered to be the source of oxygen for the spinel growth during processing and thermal loading of Al–Al_2O_3 composites [11]. In δ-Al_2O_3 fibre reinforced aluminium alloys, interaction of the alloy with the SiO_2 components of the binder and the fibre is therefore expected prior to interaction with δ-Al_2O_3. Due to the different constitution of the SiO_2 in the binder and in the fibre (probably bonded as mullite $3Al_2O_3 \cdot 2SiO_2$ [1]) the interaction speed of both components with the matrix should be different.

In the present work the interaction of the aluminium piston alloy AlSi12CuMgNi with δ-Al_2O_3 fibres and the influence of SiO_2 on this interaction is studied for as-processed composites and after a thermal treatment of 60 days at 500 °C. The main interest is directed to an understanding of the fundamentals of wetting during melt infiltration and to fibre degradation during the thermal treatment of the composite.

2. Experimental procedure

The δ-Al_2O_3 fibre reinforced AlSi12CuMgNi piston alloys were processed by squeeze casting. The fibres

0022–2461

were bonded in a preform using an SiO_2 binder. The processing details are described in [5]. The composites were investigated under two conditions: in the as-processed condition, which includes a thermal treatment at 500 °C 1/h H_2O + room temperature (r.t.) + 230 °C 5/h, and for a study of the influence of a thermal load on the interface, in a condition of an additional treatment of 500 °C for 60 days^{-1} (followed by artificial ageing for 5 h at 230 °C).

The composites were prepared for analytical transmission electron microscope (TEM) investigations in the usual way by grinding, dimpling and ion milling. TEM observations were performed in a Philips 430 electron microscope attached to a Tracor 5500 energy dispersive spectroscopy (EDX) system.

In the present paper no computer image simulation of the high resolution electron microscope (HREM) images is given. The HREM images observed in this work are, however, in agreement with images for the same imaging direction given in the literature [16–20].

The electron beam induced $MgAl_2O_4$ spinel growth described in [21] was not observed in these experiments. Contrary to the experiments in [21], in the present case the ceramic material of the fibre is completely surrounded by the metallic matrix, which favours heat and charge conduction away from the investigated sample position. No sample charging was observed and therefore no carbon coating of the sample was needed.

Spinel formation in the thermal treated samples is a frequent process [5], nevertheless it was difficult to find sample positions in the microscope with a well-orientated alumina and spinel, a nearly edge-on position of the interface and thin enough for HREM investigations. Many positions with spinels on the top of the fibre and, as will be discussed, α-alumina converted into spinel were found, but not in the complete arrangement as described in later figures, where the whole process at one position could be studied. Therefore the discussion mainly covers these results, although the optimal thickness for HREM imaging was not obtained everywhere.

3. Results

3.1. Spinel growth in as-processed composites

In the as-processed δ-Al_2O_3–AlSi12CuMgNi composites mainly structureless interfaces without any reaction products between fibre and matrix are found, Fig. 1a. At some positions, however, the interface is decorated by a few nanometer large crystals growing from the fibre surface into the matrix. Locally, remnants of the SiO_2 binder are visible. In the interface between the SiO_2 binder and the matrix similar crystals are identified. In Fig. 1b such an example, with remnants of the binder on the fibre and additional crystals, is shown. The crystals observed on the fibre surface have different chemical constitutions: some were identified containing iron, some copper [5]. In the present paper only those crystals containing magnesium are studied.

Single crystals containing magnesium observed at a structureless interface similar to that shown in Fig. 1a were imaged by HREM, Fig. 1c. The HREM structure with lattice distances of 0.46 nm for the (1 1 1) planes, the CBED (Convergent Beam Electron Diffraction) pattern (showing the single crystal spots of the [0 1 $\bar{1}$] direction) and a detection of magnesium enrichment identifies the crystal as an $MgAl_2O_4$ spinel. In most such images, the crystals do not touch the fibre surface directly. Spinel formation near the fibre surface at structureless interfaces is interpreted as a result of the reaction of magnesium segregating in the interface with the remnants of the SiO_2 binder (see Discussion).

3.2. Spinel growth in thermally treated composites

In samples treated for 60 days at 500 °C the growth of 1–2 μm large spinel crystals can be observed, as was discussed in [5]. The spinel crystals grow preferentially at positions where the α-Al_2O_3 crystals of the δ fibre reach the fibre surface. The α-alumina crystal plates are embedded at irregular positions in the δ fibre, crossing them at different angles to the fibre axis. The two parallel crystal planes are mostly the (0 0 0 1) planes of the α-Al_2O_3.

In Fig. 2a a scanning electron microscope (SEM) image of a deep etched polished section of an annealed composite is shown. From the SEM images of that polished section it can be concluded that in the δ fibre, in the neighbourhood of the spinels, pores are formed during heat treatment. The formation of these pores was interpreted as the solution of less stable parts of the fibre, such as SiO_2, during heat treatment of the composite [5].

In Fig. 2b a TEM image of a spinel on the top of the α-Al_2O_3 crystal is shown. The sample position shown in Fig. 2b was investigated in some detail and the results will be discussed in the following sections.

In Fig. 3 the tip of the spinel from Fig. 2b is shown surrounded by the aluminium matrix. The HREM image shows the (1 1 1) lattice fringes of the $MgAl_2O_4$ spinel (d = 0.46 nm). The imaging was performed in the [0 1 $\bar{1}$] direction. The sample is not sufficiently thin to give optimal HREM images. It can be seen, however, that the interfaces between the spinel crystal and the aluminium grain are nearly in a perfect crystallographic ($\bar{1}$ 1 1) and (1 1 1) plane. No steps and only a diffuse zone of atomic thickness surrounding the crystal are visible.

Fig. 4 shows the results of two EDX line scan analyses performed at positions marked in Fig. 2b. In Fig. 5, a magnesium map is shown obtained from the region of the spinel of Fig. 2b. The magnesium segregates in the aluminium grain in a large volume surrounding the spinel crystal and is diffused inside the fibre and the α-Al_2O_3 crystal. No phases containing magnesium, lattice straining or lattice defects were identified in the Al matrix in the neighbourhood of the spinel crystal.

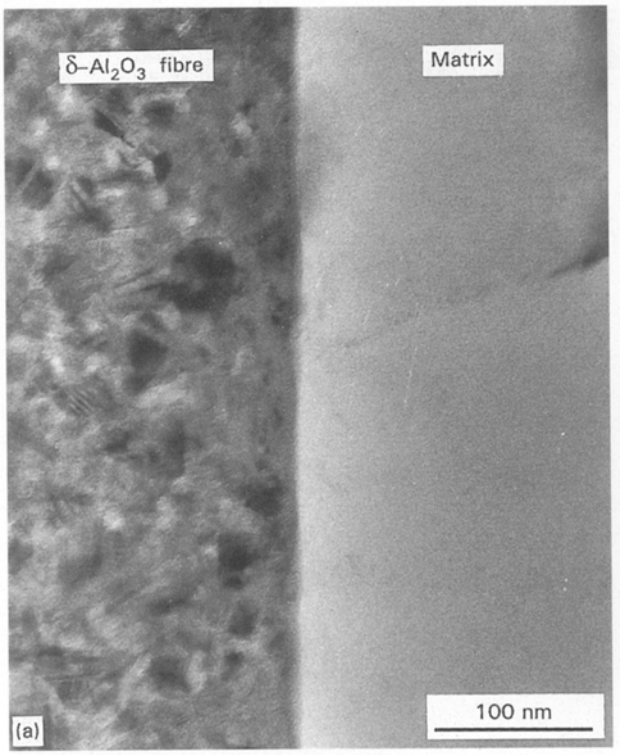

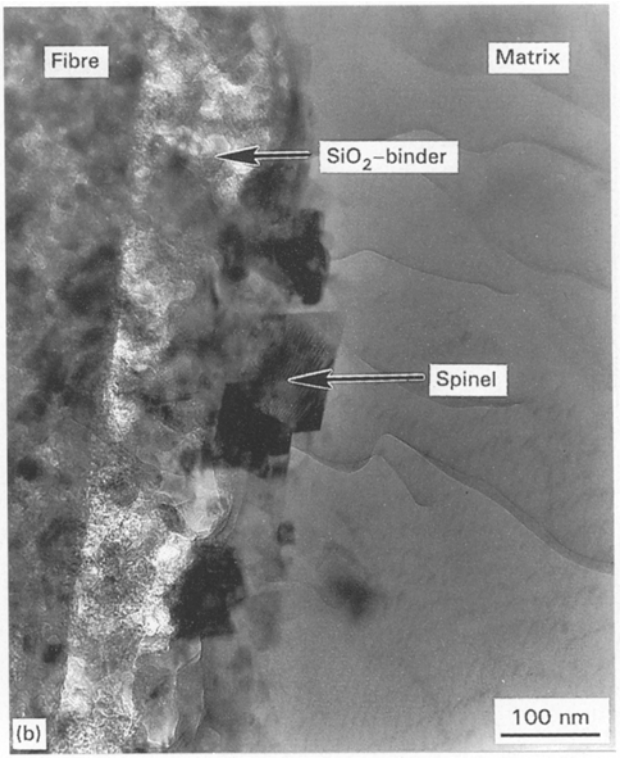

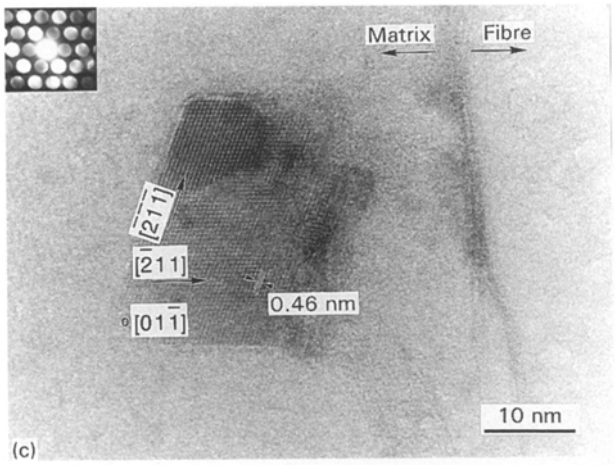

Figure 1 (a) Structureless fibre–matrix interface in an as-processed δ-Al_2O_3 fibre reinforced AlSi12CuMgNi piston alloy, (b) formation of spinels and other phases near the fibre surface covered with an SiO_2 binder layer, and (c) HREM imaging of nanometer crystals forming near the interface of as-processed δ-Al_2O_3 fibre reinforced Al piston alloy (the crystal can be identified as the $MgAl_2O_4$ spinel: imaging is performed parallel to the [0 1 $\bar{1}$] zone axis, the location of the fibre surface is marked by the two arrows defining the position of the fibre and the matrix).

As can be seen from Figs 4a and 5, at distances of approximately 100 nm from the spinel the magnesium intensity in the aluminium matrix increases and reaches its maximum inside the spinel at concentrations of roughly 20 at % (oxygen is not measured and the concentration of the elements detected is normalized to 100%). In the δ-Al_2O_3 of the fibre the magnesium intensity decreases, but increases again when the α-Al_2O_3 crystal is reached. Inside the α-Al_2O_3 crystal the same magnesium concentration of roughly 20 at %, as in the spinel, is measured. Behind the α-Al_2O_3 crystal the magnesium intensity decreases rapidly to small values. The silicon concentration near the spinel varies also. It is roughly 2 at % in the aluminium grain of the matrix near the spinel, below 1 at % in the spinel and in the α-Al_2O_3 and a few at % in the δ-Al_2O_3 fibre.

The magnesium map and the two EDX line scans show that large magnesium contents occur inside of the α-Al_2O_3 crystal. The EDX line scan of Fig. 4b was performed at a position inside the α-Al_2O_3 crystal where the magnesium content decreases to small values. This is the boundary between the reacted and the unreacted part of the α-Al_2O_3 crystal. It should be noted that inside the reacted part of the α-Al_2O_3 crystal near the reaction front, the magnesium concentration is approximately 13 at %, which is lower than the Mg concentration measured in the spinel on the top of the fibre and in the α-Al_2O_3 near the fibre surface.

Lattice imaging, CBED and the semiquantitative analysis of the elements magnesium and aluminium inside the α-Al_2O_3 in the neighbourhood of the spinel growing on the surface of the fibre proves that this part of the alumina crystal is converted into a magnesium spinel. The transformation front from the spinel to the alumina is identified by the EDX line scan of Fig. 4b, showing a drop of magnesium going from the spinel (point C) into the alumina (point D).

The interface between the α-Al_2O_3 crystal converted into the spinel and the δ-Al_2O_3 polycrystalline fibre material is shown in Fig. 6a. In Fig. 6b a similar interface of a composite in the as-processed condition is shown for comparison. The crystals are imaged in the [2 $\bar{1}$ $\bar{1}$ 0] or [0 1 $\bar{1}$] direction of the alumina and spinel, respectively. Fig. 6b shows the (0 0 0 1) planes of the α-Al_2O_3 crystal. In the as-processed condition, Fig. 6b, an atomically sharp interface is observed between the α-Al_2O_3 "monocrystal" and the

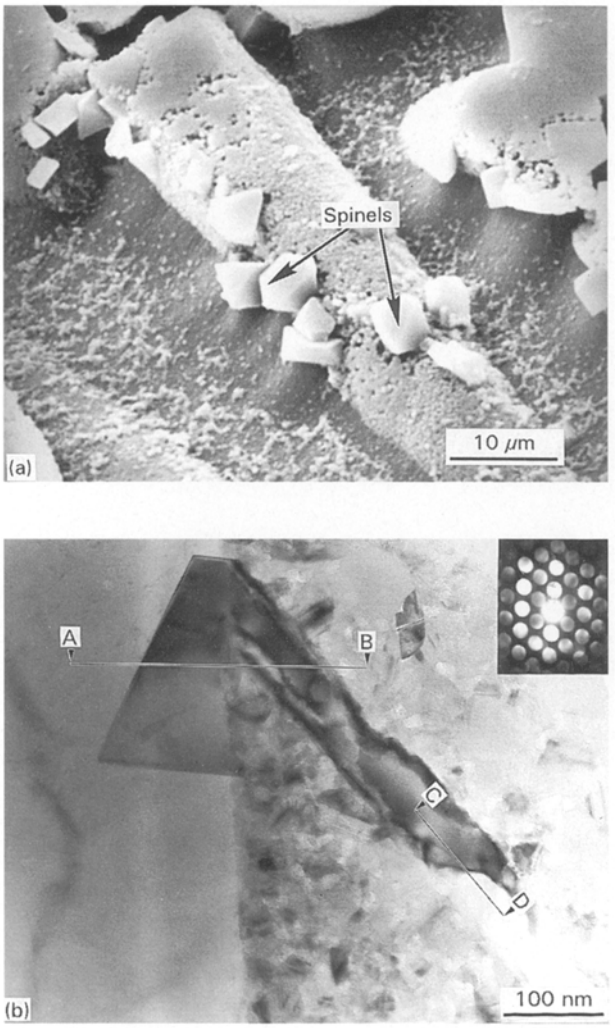

Figure 2 (a) SEM image of a deep etched polish section showing the formation of pores in the neighbourhood of spinels in the fibre surface after heat treatment of the δ-Al_2O_3–AlSi12CuMgNi composite. (b) TEM image showing the formation of large $MgAl_2O_4$ spinels on the surface of δ-Al_2O_3 fibres at positions where the α-Al_2O_3 crystals reach the fibre surface in composites treated at 500 °C for 60 days. See Fig. 4 for AB and CD.

polycrystalline δ material. In the composites treated for 60 days at 500 °C the interface is rough and strongly modified by formation of the spinel lattice.

3.3. The alumina–spinel transformation front

In Fig. 7a an HREM image is shown from the interface between the α-Al_2O_3 converted into the spinel and the unreacted α-Al_2O_3 crystal. The image shows the (1 1 1) lattice planes ($d = 0.46$ nm) of the $MgAl_2O_4$ spinel and the $(0\,\bar{1}\,\bar{1}\,2)$-planes ($d = 0.34$ nm) of the α-Al_2O_3 crystal. The electron beam direction is nearly parallel to the $[0\,\bar{1}\,\bar{1}]$ of the spinel and $[2\,\bar{1}\,\bar{1}\,0]$ of the alumina direction. The electron beam illumination, however, is not everywhere parallel to the plane of the interface. The orientation of the spinel–alumina interface in relation to the lattice of α-Al_2O_3 is not uniform for different sample positions. As can be concluded from Figs 7a and 8, the interface is nearly parallel to the following planes of the α-Al_2O_3: (0 0 0 6) left, $(0\,1\,\bar{1}\,2)$ middle and $(0\,\bar{1}\,1\,4)$ right part of Fig. 7a.

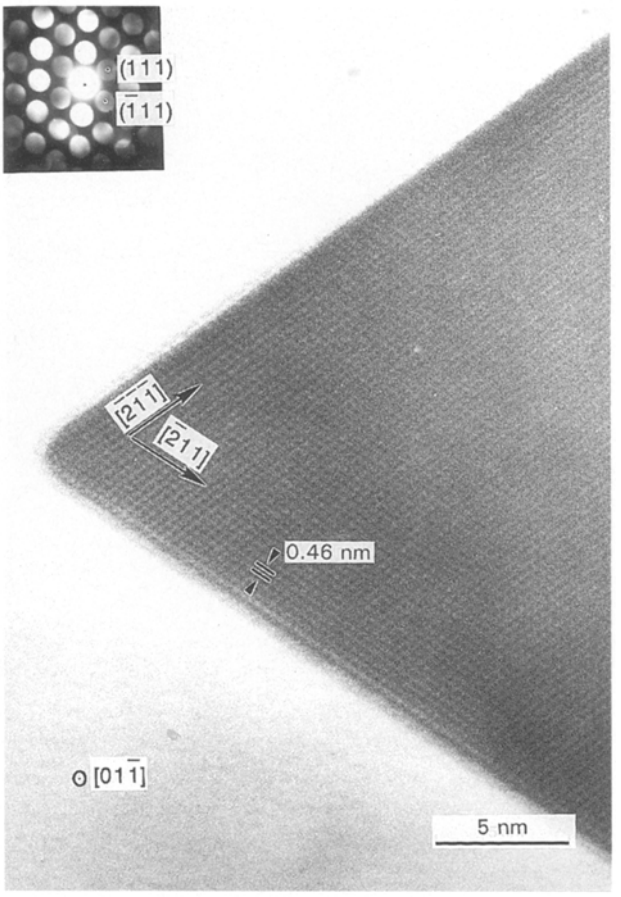

Figure 3 HREM image of the tip of the $MgAl_2O_4$ spinel shown in Fig. 2a. (1 1 1) lattice planes with imaging direction $[0\,1\,\bar{1}]$.

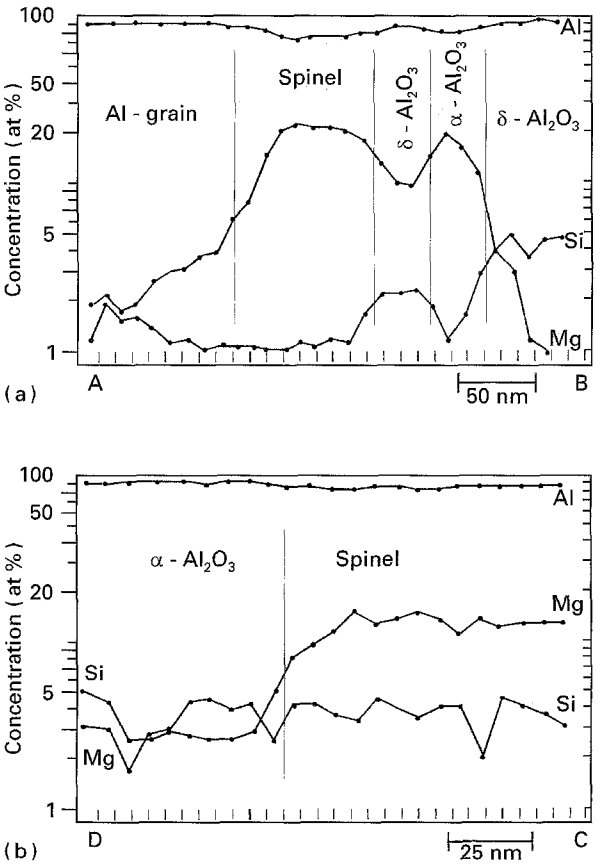

Figure 4 EDX-line scan across (a) the spinel perpendicular to the interface AB as shown in Fig. 2a, and (b) the reaction front α-Al_2O_3–spinel CD as shown in Fig. 2a.

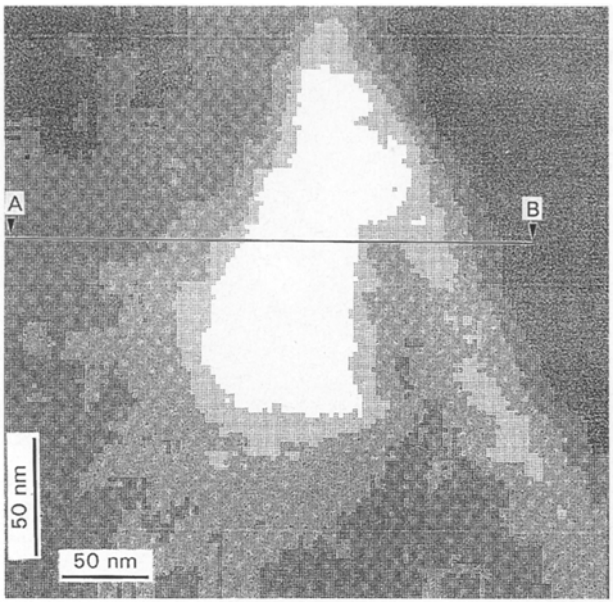

Figure 5 Magnesium element distribution map in the region of the spinel shown in Fig. 2a. Bright marks indicate regions of high magnesium concentration.

As can be deduced from the images of Figs 7a and 8, due to the transformation of the alumina into the spinel, the lattice direction $[0\bar{1}\,1\,1]$ of α-Al_2O_3 changes into the direction $[\bar{2}\,\bar{1}\,1]$ of the spinel by an inclination of approximately 13°. The reaction front has a thickness of less than 5 nm. At many positions the two lattices are touching nearly at the atomic scale, as shown in Fig. 8. The number of lattice planes of the spinel can be correlated to that number of the α-Al_2O_3 lattice and a ratio of three planes in the spinel correlates to approximately four of the alumina.

In Figs 7a and 8 the reaction front is not clearly defined as a phase boundary, as is the case for example in reaction experiments between a divalent and a trivalent oxide [22]. As can be concluded from Fig. 7b, which shows an image from another position of the same reaction front, parts of alumina locally are converted into a spinel without forming a defined phase interface. The reaction proceeds obviously by local diffusion of magnesium through the lattice of α-Al_2O_3. Transformation of alumina into spinel takes place locally without formation of a homogeneous phase boundary.

4. Discussion

4.1. Formation of the spinel

Spinel formation is usually investigated by a reaction of two oxides with a divalent and a trivalent cation. Temperatures between 1500 [18] and 1900 °C [21, 23] are typically applied to simulate this reaction. A reaction zone consisting of a spinel of a few tens of micrometers is obtained in this case in a few hours. The mechanism of spinel formation at these temperatures is interpreted as counterdiffusion of the cations through the rigid oxygen sublattice at both interfaces, Al_2O_3–$MgAl_2O_4$ and $MgAl_2O_4$–MgO [24–27]. Three Mg^{2+} ions have to diffuse inward for every two Al^{3+} ions diffusing outward to preserve charge

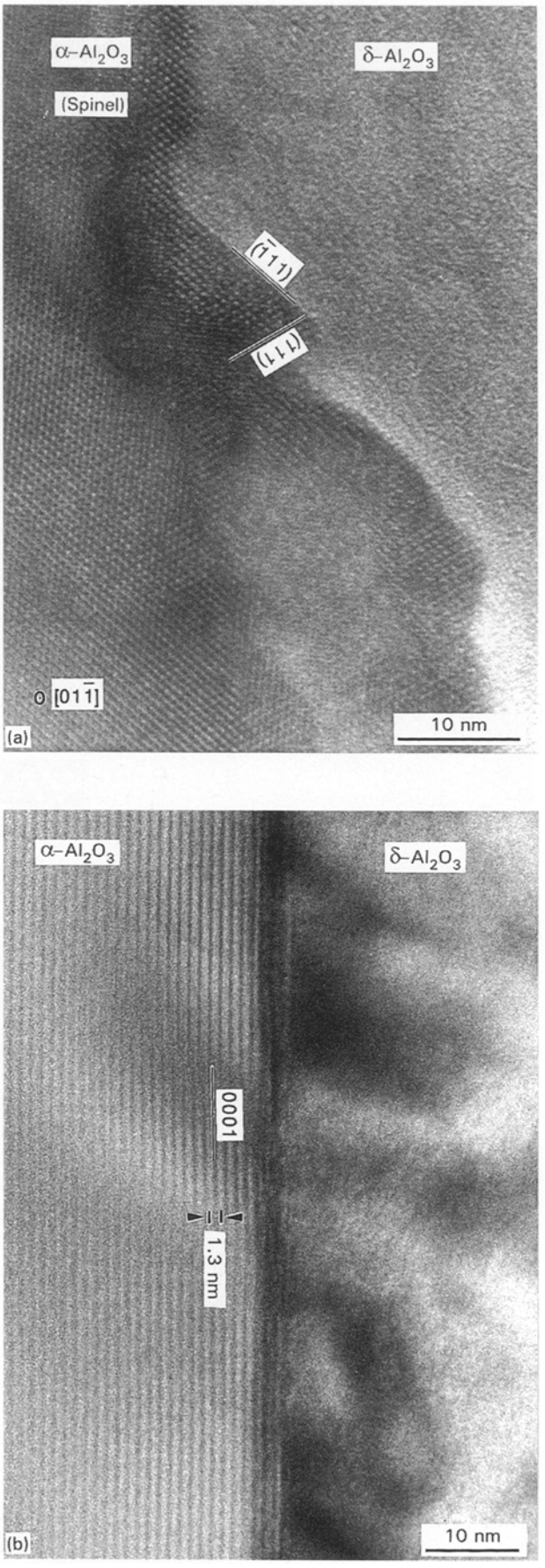

Figure 6 Interface between the α-Al_2O_3 crystal and the polycrystalline δ-Al_2O_3 fibre for (a) composite treated at 500 °C for 60 days, and (b) as-processed composite (the lattice fringes show the (0 0 0 1) planes, imaging direction is $[2\,\bar{1}\,\bar{1}\,0]$).

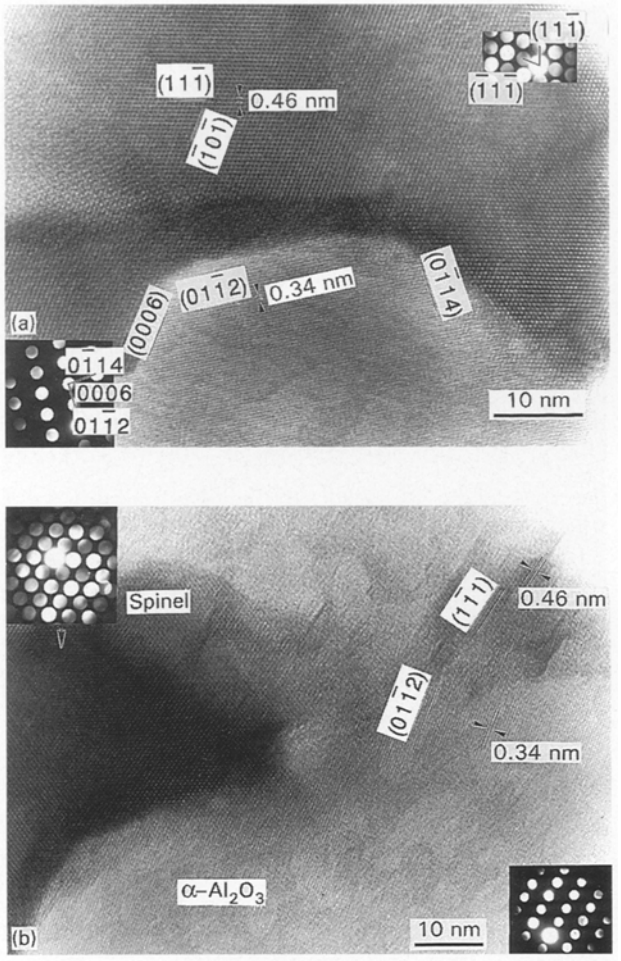

Figure 7 (a) Transformation front between the spinel and alumina in the composite treated at 500 °C for 60 days (imaging near [0 1 $\bar{1}$] and [2 $\bar{1}$ $\bar{1}$ 0] directions of the α-alumina and spinel, respectively), and (b) showing the local transformation of alumina into spinel probably due to a higher magnesium segregation (no clear phase boundary can be identified).

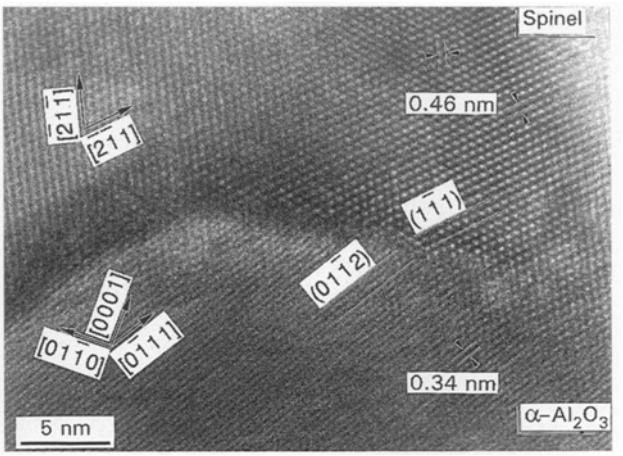

Figure 8 Details of the reaction front between alumina converted into the spinel and alumina crystal of the fibre. The diffraction diagrams (Fig. 7a) are in the correct orientation to the lattice planes.

balance in the spinel. In [21] the reaction of an MgO layer with the alumina surface induced by electron irradiation was observed. According to the authors, the reaction is controlled by charge neutralization of cations during electron irradiation. The reaction temperature was not known in this case. For the Ni–Al_2O_3 interface it was shown that spinel formation can take place without the formation of a nickel oxide layer. The spinel formation will take place at temperatures above 1000 °C when an oxygen concentration in the nickel above a threshold value is reached [28].

The transformation of the h.c.p (hexagonal close-packed) lattice of α-Al_2O_3 into the face centred cubic (f.c.c.) lattice of the spinel probably involves two steps [25]. In the first step, a change of anion layer sequence from hcp to fcc by a correlated motion involving dislocation takes place. In the second step, a redistribution of the cations follows.

During squeeze casting of δ-Al_2O_3 fibre reinforced aluminium piston alloys, which is performed near the melting temperature of the aluminium alloy (770 °C, [5]), small spinel crystals grow near the fibre–matrix interface. The location of the crystals at some distance from the fibre makes it likely that the spinel formation results from reaction of the remnants of the SiO_2 binder with the magnesium segregating in the interface. The formation of such spinels at interfaces with a high content of SiO_2 binder, as shown in Fig. 1b, is another argument in favour for that assumption. At processing temperatures, the incubation time for the formation of a spinel as a result of reaction between magnesium and alumina is of the order of 2000 s according to [10]. The formation of spinel as a result of the reaction of magnesium with SiO_2, on the other hand, follows from thermodynamical considerations and was also observed experimentally [11, 29, 30].

Under the heat treatment conditions of 500 °C for 60 days, studied in this work, the conversion of α-alumina crystals into spinel proceeds at distances of roughly 0.3 μm. The spinel crystal growing on the top of the fibre in Fig. 2b is of the same order. Contrary to diffusion experiments with two oxides for spinel formation, in the present case the interaction takes place between an aluminium grain enriched with magnesium and the alumina of the fibre at much lower temperatures.

The large magnesium spinel crystals observed in composites treated at 500 °C for 60 days grow preferentially at positions where the α-Al_2O_3 crystals reach the fibre surface. Two reactions proceed here during heat treatment: the growth of spinel from the surface of the α-Al_2O_3 crystal into the aluminium grain of the matrix, and a transformation of the α-Al_2O_3 crystal into a spinel. Assuming the aluminium matrix does not interfere with the EDX results (which is very unlikely because of the small thickness of the sample, 10 nm, as can be concluded from the feasibility of HREM imaging), for both spinels the same magnesium content of 20 at % compared to the aluminium results from the EDX analysis. This leads to a spinel of the form $MgO \cdot x \cdot Al_2O_3$, with $x = 2$, which is a typical value for artificial aluminates, where x may be between 1 and 3.5 [13, 18, 31, 32]. For the magnesium concentration nearby the alumina–spinel transformation front approximately 13 at % Mg was measured (Fig. 4b), which is near the x value of 3.5. This is in agreement with the expectation that in the neighbourhood of Al_2O_3 a spinel saturated with Al_2O_3 should form [28].

For the transformation of alumina into spinel in this work the following explanation can be considered. α-Al_2O_3 has 32 octahedral and 64 tetrahedral interstices. Two-thirds of the octahedral interstices are occupied by Al atoms. In the spinel the same interstices are present, the cations are, however, distributed on 16 octahedral and eight tetrahedral sides. Having the alumina spinel transformation in mind, α-Al_2O_3 can be rewritten as follows

$$\alpha\text{-}Al_2O_3 \rightarrow AlAl_{5/3}O_4 \rightarrow Al_8Al_{40/3}O_{32} \quad (1)$$

$Al_8Al_{40/3}O_{32}$ reacts at the interface with magnesium under the formation of spinel with an Mg concentration of 13 at %. A reaction which is in agreement with this observation is

$$Al_8Al_{40/3}O_{32} + 8/3Mg \rightarrow Al_8[Al_{40/3}Mg_{8/3}]O_{32}$$
$$/Al\,[Al_{5/3}Mg_{1/3}]O_4 \quad (2)$$

A spinel is formed in this reaction with 16 octahedral interstices occupied by Al and Mg atoms in the relation of 5:1 and the tetrahedral sides are occupied by eight Al atoms. From the atoms in the unit cell in that spinel a relation of Mg:Al = 1:8 = 12.5 at % results.

The increase of the magnesium concentration from 13 at % at the reaction front to a concentration of 20 at % in the spinel near the fibre surface may be explained by the diffusion of magnesium through the spinel lattice. Considering once more the occupation of eight tetrahedral sides by Al atoms and the 16 octahedral sides by Al and Mg atoms, a spinel with 20 at % Mg of the form

$$Al_8[Al_{10/16}Mg_{22/16}]O_{32} \rightarrow Al[Al_{5/8}Mg_{11/8}]O_4 \quad (3)$$

results. The 16 octahedral sides will be occupied by five Mg and 11 Al atoms.

For the formation of the spinel $MgO{\cdot}2{\cdot}Al_2O_3$ at the fibre surface, charge neutralization is ensured by the interaction of seven O^{2-} ions with one Mg^{2+} and four Al^{3+} ions. For a supply of seven O^{2-} ions three and a half SiO_2 molecules have to be dissociated in the matrix. From that reaction, the importance of oxygen ion supply to the matrix for spinel formation is obvious.

The atomically flat crystal of the spinel grows into the aluminium grain by condensation of the magnesium which is enriched in the neighbourhood of the spinel. (According to [33] the segregation of magnesium is chemically driven by the greater affinity of Mg atoms for oxygen.) During heat treatment of the composite the following mechanism can therefore be concluded for spinel formation. On top of the α-Al_2O_3 crystal a nucleus of spinel forms due to monolayer segregation of magnesium. The oxygen can reach the top of the spinel by diffusion through the aluminium grain or through the fibre–matrix interface [10]. (The oxygen diffusion coefficient through the alumina is very low [34].)

The formation of oxygen–metal clusters in the melt and their diffusion to the metal–ceramic interface during wetting experiments was discussed by [8, 35, 36]. This process would explain the increase of wetting and the reduction of the work of adhesion for metals with a high solubility of oxygen in the melt, such as copper, silver, nickel and iron on alumina [37]. The supply of oxygen to the fibre–matrix interface during the time of melt infiltration (1 min) is low according to [1], however. In the case of the present experiment, with annealing times of 60 days at 500 °C, a high amount of oxygen should reach the reaction front by this process. The importance of oxygen solution in metal, for spinel formation at the ceramic–metal interface, was shown in the Ni–Al_2O_3 system by [28]. An $NiAl_2O_4$ spinel will form in the interface only when sufficient oxygen is solved in nickel.

The homogeneous growth of the spinel layer by layer, as can be concluded from Fig. 3, makes it likely that the supply of oxygen and magnesium takes place through the aluminium grain and not through the interface. The authors propose that the oxygen needed to form the spinel is supplied by reduction of the SiO_2 of the binder and the SiO_2 content of the fibre and by diffusion through the aluminium matrix. As the pores in the neighbourhood of the fibre show, Fig. 2a, after consumption of the remnants of the binder, parts of the fibre are solved in the matrix supplying the spinel with oxygen [5]. Magnesium and oxygen condense, as proposed by Naidich [35], as metal–oxygen clusters, at the fibre surface at positions of spinel nucleation centres.

Spinel growth from the surface of the α-Al_2O_3 crystal into the inside of that crystal needs only a supply of magnesium. The magnesium is supplied to the reaction front by its segregation in the neighbourhood of the spinel crystal. The diffusion of magnesium inside the fibre can take place in two ways: through the α-Al_2O_3–δ-Al_2O_3 interface or through the spinel lattice. The previously sharp interface between the α-Al_2O_3 crystal and the δ-Al_2O_3 polycrystalline material of the fibre will favour the diffusion of magnesium into the fibre, and the transformation of α-Al_2O_3 into the spinel may therefore proceed from that interface. As can be concluded from Fig. 7b magnesium will also diffuse through the alumina lattice, however.

In Fig. 9, the solid–solid reaction for the spinel formation in this work is shown schematically. After processing, Fig. 9a, only a monolayer of magnesium was segregated in the fibre–matrix interface [3, 4]. After heat treatment at 500 °C for 60 days a spinel was formed by the two reactions: (i) spinel growth from Al and segregation of Mg and O in the matrix, and (ii) transformation of α-Al_2O_3 into spinel by the diffusion of magnesium into the alumina lattice.

4.2. Alumina–spinel transformation model

For explanation of the transformation of α-Al_2O_3 into spinel the model shown in Fig. 10a is proposed. The two lattices of alumina and spinel are shown in the projection observed in the HREM image of Fig. 8. In Fig. 10a are shown the positions of the Al, Mg and O atoms in the lattice as explained in the legend and of the HREM image bright spots by large circles. The large circles are also the positions of the vacancies in α-Al_2O_3 and the positions of the magnesium atoms in

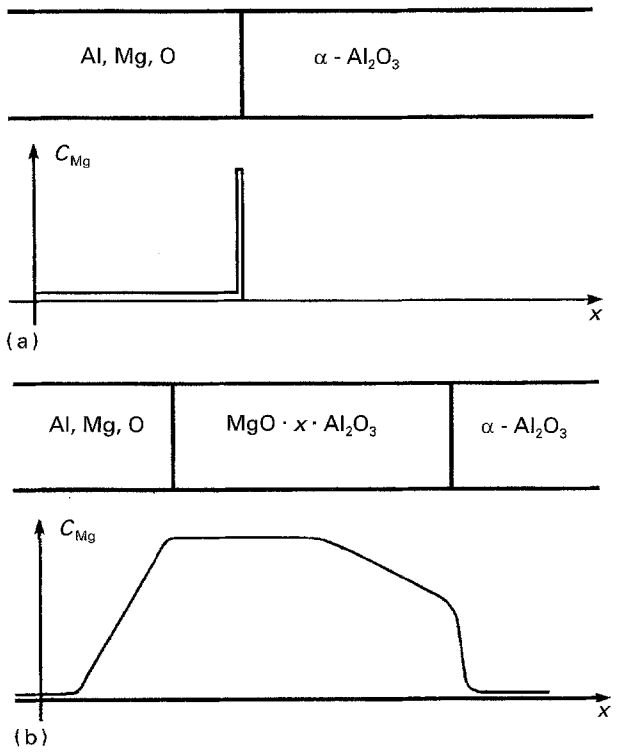

Figure 9 Schematic representation of the spinel formation due to a solid–solid reaction: (a) after processing, and (b) after thermal treatment at 500 °C for 60 days with increasing Mg concentration, C_{Mg}.

the (stoichiometric) spinel. Similar lattice descriptions with the same imaging direction proved by computer image simulation of alumina and spinel are given in [16, 19, 20] and [17, 18], respectively.

During the transformation of alumina into spinel a change of the lattice orientation is observed by different authors. According to [17] the $NiAl_2O_4$ spinel–alumina interface exhibits a 9° rotation between the {1 1 1} and the (0 0 0 1) planes of the spinel and alumina, respectively. For the $CoAl_2O_4$ spinel in [18] different small rotations of a few degrees between the (1 1 1) planes of the spinel and the (0 0 0 1) plane of the alumina were found.

As can be concluded from the model of Fig. 10a, the lattice direction $[0\,\bar{1}\,1\,1]$ of α-Al_2O_3 changes into the lattice direction $[\bar{2}\,\bar{1}\,1]$ of spinel by a rotation of an angle of 13°. For every fourth $(0\,1\,\bar{1}\,2)$ lattice plane with the $[0\,\bar{1}\,1\,1]$ direction of α-Al_2O_3 a continuous transition into the $[\bar{2}\,\bar{1}\,1]$ lattice direction of the spinel is observed and this is realized for every third of the $(1\,\bar{1}\,1)$ lattice planes in the $[\bar{2}\,\bar{1}\,1]$ direction of the spinel. The observed sequence of alumina and spinel planes can be explained by the lattice correlation shown in Fig. 10b, in which the interface of the alumina and spinel is parallel to the directions $[0\,\bar{8}\,8\,1]$ and $[0\,\bar{1}\,1]$, respectively. For this direction an agreement results for the distance AB between the vacancies of every fourth $(0\,1\,\bar{1}\,2)$ plane of alumina and the magnesium position in every third $(1\,\bar{1}\,1)$ plane of the spinel. The lattice rotation of 13° observed in Fig. 8 results therefore due to the identity of distances for some vacancies in alumina with some positions of magnesium in the spinel.

The transformation front of the α-alumina into the spinel was observed in Fig. 7a to be nearly parallel to the planes $(0\,1\,\bar{1}\,2)$, (0 0 0 1) and $(0\,1\,\bar{1}\,4)$ of α-Al_2O_3. As can be concluded from Fig. 10a these planes have the highest density of vacancy in α-Al_2O_3. The fact that the transformation front is nearly parallel to planes with a high density of vacancies and that the 13° rotation is connected with the identity of some vacancy positions in α-Al_2O_3 with the position of the magnesium atoms in the spinel, shows that the vacancies in α-alumina and probably the diffusion of magnesium atoms along the paths of these vacancies play a major role in the alumina–spinel transformation in these experiments.

In Fig. 10c, the model of the lattice is shown once more, however, the spinel–fibre–alumina region of Fig. 2b is introduced by correlating the lattice orientation of the alumina crystal as observed in Fig. 8 to the model of Fig. 10a. The α-Al_2O_3 crystal is embedded into the δ fibre, with large crystal boundaries parallel to the (0 0 0 1) lattice planes of α-Al_2O_3. A clear correlation is proved between the spinel crystal orientation growing on the fibre surface, and the lattice of the spinel in the reaction front between α-Al_2O_3 and the spinel inside the fibre. From this observation it follows that the same correlation of lattices observed inside the fibre between the alumina and the spinel will also be realized at the surface of the fibre for the spinel growing into the aluminium grain of the matrix. Both spinels, the one on top of the fibre and the other, growing by transformation from the α-Al_2O_3 form one large crystal with uniform orientation of the lattice.

From the Fig. 10c one also obtains the crystallographic plane of the α-Al_2O_3 crystal in the fibre surface exposed to the metal during infiltration before thermal treatment was applied. It is the $(0\,1\,\bar{1}\,4)$ plane. As can be concluded from Fig. 10c, in this plane a high concentration of vacancies in the α-Al_2O_3 crystal is present. During melt infiltration and magnesium segregation in the fibre–matrix interface the vacancies in the $(0\,1\,\bar{1}\,4)$ plane will therefore be first occupied by magnesium atoms. The preferential growth of spinel on the surface of the fibre at positions where the α grains reach the fibre surface takes place at lattice planes with a high density of vacancies in α-Al_2O_3.

4.3. Wetting mechanism

From the detection of magnesium [3, 4] and proof of the lattice structure of the spinel by electron diffraction [2] in the interface it was concluded [1] that wetting and adhesion in Al_2O_3–AlMg alloys is promoted by spinel formation at the interface. Observation of nanometer scale spinel crystals in the interface in these experiments in the as-processed composites may explain the observed electron diffraction diagrams of the spinel in [2]. The formation of spinels in the as-processed composites observed in the present work has no influence on adhesion at the interface, however. Wetting and adhesion is conducted by the development of mono-atomic bondings between the metal and ceramic and there is no need of the development of "mono-atomic" layers of a compound like

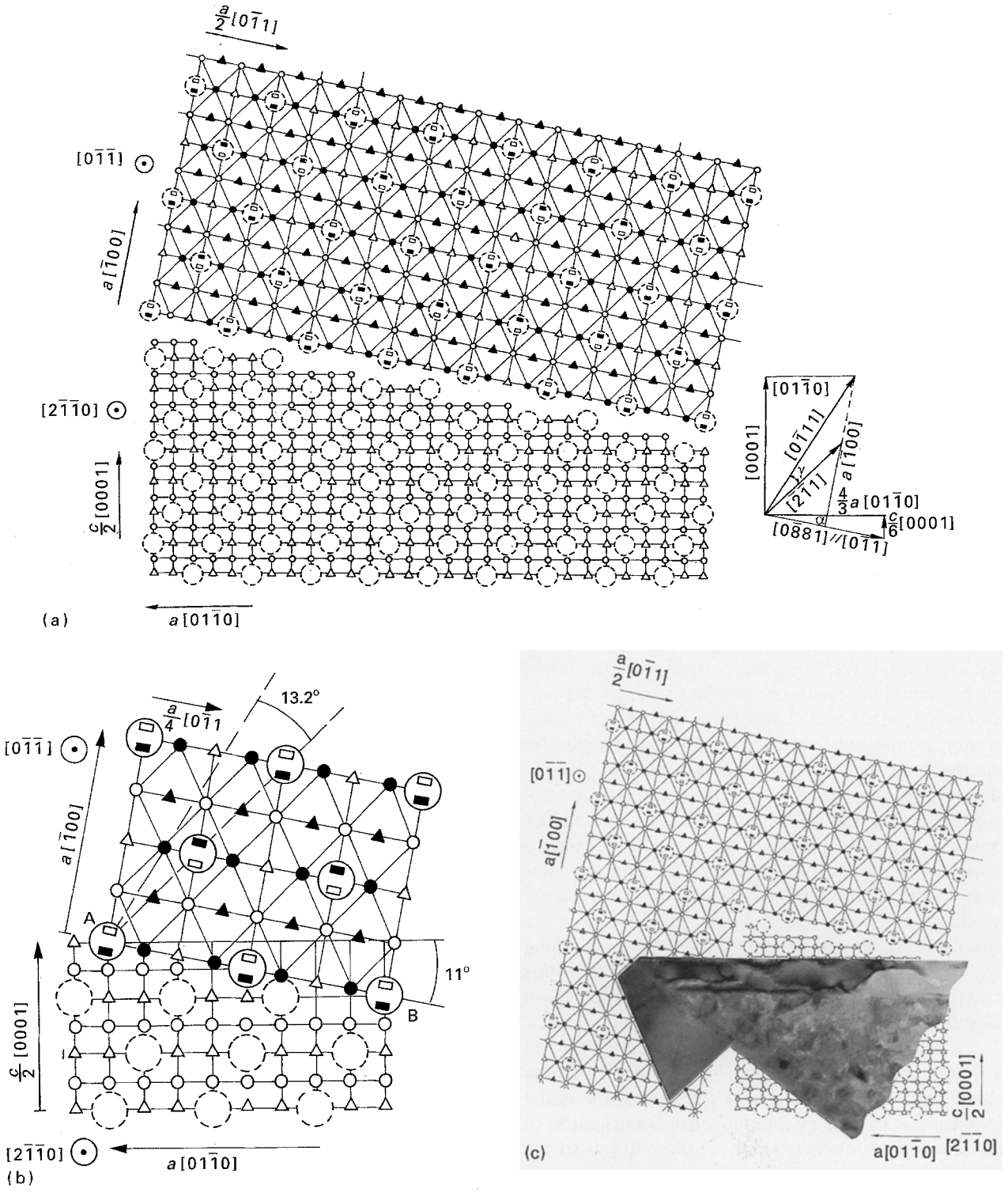

Figure 10 (a) Crystallographic model explaining the transformation front of Fig. 8. The large circles mark the positions of the vacancies in the α-alumina and the magnesium atom positions in the spinel, (b) Shows the correlation of the lattices of the α-Al_2O_3 crystal and the spinel during alumina–spinel transformation. The large circles mark the positions of the vacancies in the α-alumina and the magnesium atom positions in the spinel. (c) Shows the correlation between the observed spinel crystal and the lattice model demonstrating the initial nucleation of the spinel on the surface of the fibre in vacancies of the α-Al_2O_3 crystal. Interface fibre matrix parallel to the (0 1 $\bar{1}$ 4) plane of the α-alumina. Oxygen: (○) plane 1, (●) plane 2. Aluminium: (△) plane 1, (▲) plane 2. Magnesium: (□) plane 1, (■) plane 2.

spinel [38, 39]. The wetting and adhesion is, however, increased by segregation of some alloying elements at the interface. Spinel formation at the interface is a secondary effect connected with fibre–matrix reaction during prolonged heat treatment.

From the present observations the mechanisms of wetting, adhesion and fibre-matrix reaction can be concluded in the particular case of orientation of alumina in aluminium–magnesium alloys. During melt infiltration magnesium segregates in the fibre–matrix interface and will especially take off vacancy positions near the surface of alumina. Wetting and adhesion are increased by this effect [38]. During the following heat treatment, magnesium diffuses into the alumina taking off the positions of vacancies from which the transformation of alumina into spinel is

initiated. At the same time, more magnesium segregates in the interface and together with the oxygen solved in the aluminium matrix the spinel grows into the aluminium matrix.

5. Conclusions

In the studied system of alumina fibre reinforced piston alloys, fibre degradation during heat treatment of the composites is a consequence of reaction of the magnesium segregating in the fibre–matrix interface forming a spinel. For spinel formation oxygen is needed, which is taken from the oxygen solved in the aluminium matrix. This favours the solution of SiO_2 remnants of the binder and SiO_2 components of the fibre in the matrix. Fibre degradation can be reduced when a sufficiently high concentration of oxygen donor is present in the composite. This role may be taken by the SiO_2 binder in this case [38].

From the present investigations, wetting, adhesion and fibre–matrix reaction mechanisms in the Al_2O_3 fibre reinforced aluminium alloys can be understood by the following considerations. The formation of nanometer scale large spinel crystals near the interface indicates that spinel formation during the melt infiltration process takes place rather as small crystals and not as a monolayer. The good wetting and adhesion of pure aluminium melts on alumina at high temperatures is another hint that there is no need of monoatomic compound formation for the development of interfaces in metal–matrix composites. The magnesium segregation in the fibre–matrix interface promotes wetting and adhesion by taking off vacancy positions in the surface of the fibre. The vacancy positions in the fibre are, however, for some orientations of the alumina a nucleus for growth of reaction products, for which less stable parts of the fibre are dissolved. At the same time vacancies in the alumina are positions where diffusion of magnesium atoms into the fibre take place which result in transformation of alumina into spinel.

The nucleation of spinel preferentially on top of an α-Al_2O_3 crystal and the transformation of alumina into spinel shows that fibre degradation by spinel formation is caused by inhomogeneous nucleation of the reaction products (similar to observations in the Mg–α-Al_2O_3 system [40]) on some crystallographic orientations of α-Al_2O_3 and probably also γ-Al_2O_3 (γ-Al_2O_3 has a lattice structure similar to that of spinel [32]). As a consequence, fibre passivation cannot be obtained by the growth of a homogeneous reaction layer, as was postulated in [41] from thermodynamical considerations.

A reduction of the fibre matrix reaction speed can be obtained in the authors' understanding by a reduction of the α-Al_2O_3 content of the δ fibre. The amount of SiO_2 in the fibre may remain unchanged, as long as a sufficiently high content of SiO_2 binder or another less stable oxygen donor is present. α-Al_2O_3 fibres can be used for reinforcement when the vacancies on the fibre surface are filled by atoms not diffusing inside the alumina and preventing inhomogeneous nucleation of reaction products between fibre and matrix [38, 39].

Acknowledgements

The authors wish to thank Dr G. Neite, Metallgesellschaft AG Frankfurt, for processing the composite material and Professor W. A. Kaysser, DLR Köln for kind support of this work.

References

1. G. R. CAPPLEMAN, J. F. WATTS and T. W. CLYNE, *J. Mater. Sci.* **20** (1985) 2159.
2. A. MUNITZ, M. METZGER and R. MEHRABIAN, *Met. Trans.* **A10** (1979) 1491.
3. C. G. LEVI, G. J. ABBASCHIAN and R. MEHRABIAN, *ibid.* **A9** (1978) 697.
4. H. J. DUDEK, *Mater.-wiss. Werkstofftech.* **21** (1990) 48.
5. H. J. DUDEK, R. BORATH, A. KLEINE and G. NEITE. *Mater. Sci. Engng* **A167** (1993) 129.
6. P. D. OWNBY, KE WEN K. LI and D. A. WEIRAUCH Jr, *J. Amer. Ceram. Soc.* **74** (1991) 1275.
7. J. LI, *Rare Metals* **10** (1991) 255.
8. D. CHATAIN, L. COUDURIER and N. EUSTATHOPOULOS, *Revue Phys. Appl.* **23** (1988) 1055.
9. Z. LIJUN, W. JIMBO, Q. JITING, N. QIU and Q. PEIXIANG, in "Interfaces in Metal–Ceramic Composites", edited by R. Y. Lin, R. J. Arsenault, G. P. Martins, S. G. Fishman (The Minerals, Metals and Materials Society-Publication, 1989) pp. 213–226.
10. A. D. McLEOD and C. M. GABRYEL, *Met. Trans.* **23A** (1992) 1279.
11. NING WANG, ZHIRUI WANG and G. C. WEATHERLEY, *ibid.* **A23** (1992) 1423.
12. O. KUBASCHEWSKI and C. B. ALCOCK, "Metallurgical Thermochemistry", 6th Edn (Pergamon, Oxford, 1993) p. 242.
13. W. D. KINGERY, H. K. BOWEN and D. R. UHLMANN, "Introduction to Ceramics" (Wiley, New York, 1976) p. 991.
14. K. PRABRIPUTALOONG and M. R. PIGGOTT, *J. Amer. Ceram. Soc.* **121** (1973) 184.
15. P. D. OWNBY, K. W. K. LI and D. A. WEIRAUCH Jr, *ibid.* **74** (1991) 1275.
16. W. MADER, *Z. Metallkd.* **83** (1992) 478.
17. Y. K. SIMPSON, S. McKERNAN and C. B. CARTER, *J. Amer. Ceram. Soc.* **70** (1987) C141.
18. C. B. CARTER and H. SCHMALZRIED, *Phil. Mag.* **A52** (1985) 207.
19. D. KNAUSS and W. MADER, *Ultramicrosc.* **37** (1991) 247.
20. M. RÜHLE, *Fresenius J. Anal. Chem.* **341** (1991) 369.
21. D. X. LI, P. PIROUX, A. H. HEUER, S. YADAVALLI and C. P. FLYNN, *Phil. Mag.* **A65** (1992) 403.
22. C. B. CARTER, *Ber. Bunsenges. Phys. Chem.* **90** (1986) 643.
23. W. P. WHITNEY, and V. S. STUBICAN, *J. Phys. Chem. Solids* **32** (1971) 305.
24. R. E. CARTER, *J. Amer. Ceram. Soc.* **44** (1961) 116.
25. C. N. R. RAO and J. GOPALAKRISHNAN, in "New Directions in Solid State Chemistry", edited by R. W. Cahn, E. A. Davis and I. M. Ward (Cambridge University Press, 1988) pp. 421–501.
26. H. SCHMALZRIED, *Reactivity of Solids* **8** (1990) 247.
27. D. H. LINDSLEY, in "Oxide and Minerals", Reviews in Mineralogy Vol. 3, edited by D. Rumble III (Mineralogical Society of America, Blacksburg, VA, 1976) pp. L1-L88.
28. K. P. TRUMBLE and M. RÜHLE, *Z. Metallkde.* **81** (1990) 749.
29. Y. LE PETITCORPS, J. M. QUENISSET, G. LE BORGNE and M. BARTHOLE, *Mater. Sci. Engng* **A135** (1991) 37.
30. D. J. TOWLE and C. M. FRIEND, *J. Mater. Sci.* **27** (1992) 2781.
31. B. HALLSTEDT, *J. Amer. Ceram. Soc.* **75** (1992) 1497.
32. A. IBARRA, R. VILA and M. J. de CASTRO, *Phil Mag. Lett.* **64** (1991) 45.

33. S. O. SAIED and J. L. SULLIVAN, *J. Phys. Condens. Matter* **5** (1993) A165.
34. J. D. CAWLEY, J. W. HALLORAN and A. R. COOPER, *J. Amer. Ceram. Soc.* **74** (1991) 2086.
35. V. YU. NAIDICH, in "Progress in Surface and Membrane Science", Vol. 14, edited by D. A. Candehead and J. F. Danielli (Academic Press, New York, 1981) p. 353.
36. F. DELANNAY, L. FROYEN and A. DERUYTTERE, *J. Mater. Sci.* **22** (1987) 1.
37. S. P. MEHROTRA and A. C. D. CHAKLADER, *Met. Trans.* **16B** (1985) 567.
38. H. J. DUDEK, in "Advanced Aerospace Materials", edited by H. Buhl (Springer Verlag, Berlin, 1992) pp. 139–152.
39. *Idem*, in "Metallische Verbundwerkstoffe", edited by K. U. Kainer (DGM-Verlag, Oberursel, 1994) pp. 117–138.
40. M. PFEIFER, J. M. RIGSBEE and K. K. CHAWLA, *J. Mater. Sci.* **25** (1990) 1563.
41. B. HALLSTEDT, Z.-K. LIU and J. AGREN, *Mater. Sci. Engng.* **A129** (1980) 135.

Received 1 February 1994
and accepted 22 June 1995